In the ultra-clean limit, $l \to \infty$, we may neglect the 1 factor in Eq. (27) as compared to $(\epsilon\tau)^2$. For niobium at 0 °K, $p_F\xi \simeq 100$ and if we take $\mu = 30$ as an upper bound for μ, we obtain a ratio $l/\xi \simeq 10$. For this value of μ, the terms neglected in $\mathcal{P}_{xx}$ are of order 0.003 and those for $\mathcal{P}_{yx}$ of order 0.1. Our theory is therefore valid for l/ξ ranging from ∞ to about 10.

For $l/\xi \sim 10$, $\tau \simeq 1/30$ so that $1 + (\tau\epsilon)^2 \simeq 1$. In Fig. 1, we plot H_{eff}/H_{c2} versus $h(0)/H_{c2}$ for $\omega_{c2}\tau = 0$ and ∞, where $\omega_{c2} = eH_{c2}/mc$. For niobium $h(0)/H_{c2} \simeq 0.75$ and we have nearly $\tan\alpha = \omega_{c2}\tau$, which agrees with the experiment of Maxfield.[11]

Our calculation is performed in a frame at rest with the vortex. In this frame, the impurity scatters are moving at a velocity v_L. Our neglect of this fact probably introduces errors of order v_L/v_F which are clearly negligible.

ACKNOWLEDGMENT

I wish to thank Professor J. Bardeen for suggesting this problem and for pointing out errors in earlier versions of the manuscript.

*Research supported in part by the Advanced Research Projects Agency under Contract No. SD-131.

[1]J. Bardeen and M. J. Stephen, Phys. Rev. 140, A1197 (1965).

[2]P. Nozières and W. F. Vinen, Phil. Mag. 14, 667 (1966).

[3]C. Caroli and K. Maki, Phys. Rev. 164, 591 (1967).

[4]K. Maki, Progr. Theoret. Phys. (Kyoto) 41, 902 (1969).

[5]K. Maki (unpublished).

[6]Y. B. Kim, C. F. Hempstead, and A. R. Strnad, Phys. Rev. 139, A1163 (1965).

[7]A. K. Niessen and F. A. Staas, Phys. Letters 15, 26 (1965).

[8]W. A. Reed, E. Fawcett, and Y. B. Kim, Phys. Rev. Letters 14, 70 (1965).

[9]F. A. Staas, A. K. Niessen, and W. F. Druyvesteyn, Phys. Letters 17, 231 (1965).

[10]A. K. Niessen, F. A. Staas, and C. H. Weijsenfeld, Phys. Letters 25A, 33 (1967).

[11]B. W. Maxfield, Solid State Commun. 5, 585 (1967).

[12]A. A. Abrikosov, L. P. Gor'kov, and I. E. Dzyaloshinski, *Methods of Quantum Field Theory in Statistical Physics* (Prentice-Hall, Englewood Cliffs, N. J., 1963), p. 308.

[13]Note that the exact expression for Eq. (6) contains $\nabla - ieA_0/c$, but the term in A_0 is completely negligible as compared to ∇ in our gauge.

[14]R. M. Cleary, Phys. Rev. B 1, 169 (1970).

[15]A. L. Fetter, Phys. Rev. 140, A1921 (1965).

[16]C. Caroli and J. Matricon, Physik Kondensierten Materie 3, 380 (1965).

[17]R. M. Cleary, Phys. Rev. 175, 587 (1968).

[18]J. Bardeen, R. Kummel, A. Jacobs, and L. Tewordt, Phys. Rev. 187, 556 (1969).

[19]E. B. Hansen, Phys. Letters 27A, 576 (1968).

[20]W. Bergk and L. Tewordt, Z. Physik 230, 178 (1969).

[21]See Ref. 12, p. 312.

PHYSICAL REVIEW B VOLUME 1, NUMBER 12 15 JUNE 1970

Orthogonalized-Plane-Wave Convergence of Some Tetrahedral Semiconductors

R. N. Euwema and D. J. Stukel
Aerospace Research Laboratories, Wright-Patterson Air Force Base, Ohio 45433
(Received 9 October 1969)

The orthogonalized-plane-wave (OPW) series convergence up to 900 OPW's is illustrated for equal-core-size compounds C, Si, ZnSe, and CdTe, for large-cation-small-anion compounds ZnO, AlN, and ZnS, and for large-anion-small-cation compounds BAs, BeTe, and ZnTe. Herman's overlapping-free-atom-potential model is used primarily, although self-consistent OPW convergence results are given for BAs. It is found that the first row of the Periodic Table is exceedingly difficult to handle with the OPW formalism. The primary factors involved in OPW convergence are found to be the presence or absence of core functions in the OPW's (which was realized long ago) and the relative core sizes of anion and cation. Criteria are given for estimating the OPW convergence behavior of compounds.

I. INTRODUCTION

A number of different techniques have been developed to calculate the energy-band structure of crystals. The best-known techniques are the augmented-plane-wave[1] (APW), Korringa-Kohn-Rostoker[2] (KKR), and the orthogonalized-plane-

wave[3,4] (OPW) methods. Each technique has advantages and disadvantages which may vary in importance in different parts of the Periodic Table. In the APW and KKR techniques, the space in a crystal is divided into spheres centered on the atomic cores and the space between these spheres. A spherically symmetric potential is usually assumed within the spheres and a constant potential is assumed outside the sphere – the "muffin-tin" potential. The OPW method divides electron states rather than space. It assumes deep tightly bound nonoverlapping "core" states and loosely bound "valence and conduction" states. A spherically symmetric potential is assumed only for the core states. The valence and conduction states are expanded in a modified Fourier series of reciprocal-lattice vectors.

Systematic studies of the advantages and disadvantages of the various techniques should be made. For example, the validity of the muffin-tin approximation should be critically examined for various types of crystals. The OPW technique has the strong advantage of relative simplicity. The valence and conduction wave functions are defined in all regions by the same expression. The valence contribution to the crystalline potential need not be spherically symmetrized in the core regions. The OPW technique is probably the easiest technique to make self-consistent. Its greatest weakness involves the slow convergence of the OPW series.

The purpose of this paper is critically to examine the OPW series convergence for diamond, zinc-blende, and wurtzite semiconductors whose constituents are taken from that part of the Periodic Table shown in Table I. We will present detailed results on the ten compounds listed in Table II. These compounds were chosen to study relative anion-cation core size and the effect of the absence of core p states in the first-row elements. We have found the illustrations and criteria established in this paper to be very useful when planning OPW calculations on new compounds.

TABLE I. That portion of the Periodic Table is shown which is relevant for this paper, together with the last atomic state which is generally considered a core state in OPW calculations for that row of the table.

Atoms					Outer core state
4 Be	5 B	6 C	7 N	8 O	1s
12 Mg	13 Al	14 Si	15 P	16 S	2p
30 Zn	31 Ga	32 Ge	33 As	34 Se	3d
48 Cd	49 In	50 Sn	51 Sb	52 Te	4d

TABLE II. Compounds discussed in this paper are shown classified by their relative cation-anion size.

Relative core sizes
Same-size cores
C (no p states in core)
Si
ZnSe
CdTe
Larger cation with small anion
ZnO (no O p state in core)
AlN (no N p state in core)
ZnS
Larger anion with small cation
BAs (no B p state in core)
BeTe (no Be p state in core)
ZnTe

We will use Herman and Skillman's overlapping-free-atom-potential (OAP) model[5] for most of our illustrations because of its simplicity and because we can handle larger numbers of OPW's in this model. In our experience, the over-all convergence features are very similar for all OPW models. To support this, we will present results of our own self-consistent OPW (SCOPW) model.[6,7]

II. GENERAL OPW FORMALISM

In the OPW formalism, one must divide the electron states of the crystal into core and valence states. As many states as possible are designated core states. The restriction is that there must be no appreciable core overlap between neighboring atoms. If too few states are designated as core states, the convergence of the OPW series becomes very poor. The choice usually made is indicated in Table I where the outer-core state is given for the four relevant rows of the Periodic Table. The resulting core overlap is shown for ZnS in Fig. 1 where the number of core electrons outside the radius r is plotted versus r, with the Zn and S nuclei separated by their nearest-neighbor distance. The intersection of the Zn and S curves gives a common-core overlap of 0.02 electrons. Corresponding results for all ten compounds are given in Table III, together with the anion radius at which the crossing occurs and the nearest-neighbor distance. Herman-Skillman programs[8] for free atoms were used for these calculations. The results do not change appreciably when SCOPW cores are used.

The core-electron wave functions are calculated from a spherically symmetrized potential and can consequently be written in the atomiclike form

$$\varphi^c_{nlm}(r, \theta, \phi) = P_{nl(r)}/r\, Y^l_m(\theta, \phi) .$$

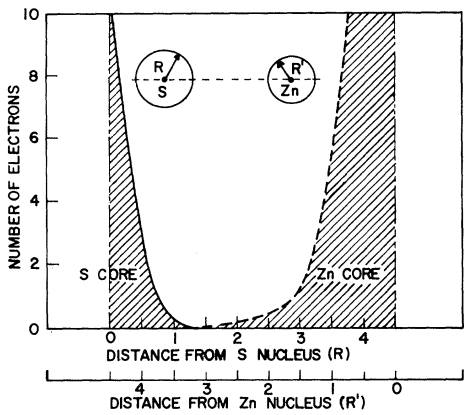

FIG. 1. Zn and S cores are shown separated by their nearest-neighbor distance (in a.u.) in ZnS. The number of core electrons outside radius r is shown.

In Herman and Skillman's OAP model, the atomic potentials (Coulomb plus exchange) due to neighboring cores are summed at each dissimilar core center. The resulting "core shifts" (given in Table III) are added to the free-atom core energies to give the core energies in the crystalline environment. In our SCOPW model, the Coulomb potential and the charge density of the valence electrons are spherically symmetrized about each inequivalent lattice site for the core calculation. Madelung terms (site-dependent constant plus parabola) are added due to the $k=0$ plane-wave charge density and the unbalanced nuclear charges. New core states are then calculated in this environment.

The valence and conduction-electron wave functions are expanded in a modified Fourier series of reciprocal-lattice vectors:

$$\psi(k_0)=\sum_{\mu} B(k_\mu)(1/\sqrt{\Omega})\,e^{ik_\mu r} - \sum_{a} e^{ik_\mu R_a}\sum_{nl} A^a_{nl}(k_\mu)\phi^a_{nl;k}(r-R_a) \ ,$$

$$k_\mu = k_0 + K_\mu \ .$$

Here k_0 gives the location in the first Brillouin zone, $\phi^a_{nl;k_\mu}$ represents a core state with quantum numbers nl, and $m=0$ when the z axis is taken in the k_μ direction. The $A_{nl}(k_\mu)$ are chosen such that each OPW is orthogonal to all core states. Thus, when a variational procedure is applied, one obtains convergence to the bottom valence state rather than to the bottom core state.

In practice, all terms in the OPW series are kept for which

$$|k_\mu| < k_{\max} = 2\pi/\lambda_{\min} \equiv \pi/r_m \ .$$

$\lambda_{\min}$ thus gives the minimum Fourier wavelength used in the series expansion. The minimum distance that can be defined with such a Fourier series is roughly

$$r_m \equiv \tfrac{1}{2}\lambda_{\min} \ .$$

Table IV gives the r_m corresponding to various numbers of OPW's for several lattice constants for the zinc-blende, diamond, and wurtzite crystal structures. r_m is directly proportional to the lattice constant, so these results are easily extended. Because k space is equally populated by reciprocal-lattice vectors, extensions can be made off

TABLE III. Compound parameters which are presented include the crystal symmetry, lattice constant (a and c for wurtzite) in Å, nearest-neighbor distance in a.u., anion and cation core shifts for Herman and Skillman's OAP model in Ry, the core-electron overlap in electrons, and the anion radius in a.u. at which there is an equal fraction of an electron (the core-electron overlap) for both anion and cation outside that radius. (D stands for diamond, W for wurtzite, and ZB for zinc blende.)

Compounds	a (Å)	Rnn (a.u.)	Anion core shift (Ry)	Cation core shift (Ry)	Core-electron overlap (electrons)	R anion (a.u.)
C (D)	3.5668	2.92	−5.734	−5.734	0.00005	1.5
Si (D)	5.431	4.44	−2.524	−2.524	0.0007	2.2
AlN (W)	3.111, 4.978	3.53	−4.841	−4.308	0.0007	1.0
ZnO (W)	3.2494, 5.2055	3.69	−2.793	−2.393	0.02	0.5
ZnO (ZB)	4.568	3.74	−2.782	−2.324	0.02	0.5
ZnS (ZB)	5.4145	4.43	−1.838	−1.750	0.02	1.2
ZnSe (ZB)	5.653	4.63	−1.586	−1.630	0.04	1.8
ZnTe (ZB)	6.07	4.97	−1.368	−1.509	0.06	2.3
CdTe (ZB)	6.482	5.30	−1.160	−1.198	0.07	2.2
BAs (ZB)	4.777	3.91	−3.070	−3.321	0.003	2.7
BeTe (ZB)	5.626	4.60	−1.845	−2.061	0.003	3.0

TABLE IV. Minimum distance r_m is shown for various numbers of OPW's for three zinc-blende lattice constants (in Å) and two wurtzite values of the c lattice constant. An ideal wurtzite c/a ratio was assumed. r_m is directly proportional to the lattice constant.

Zinc blende or Diamond				Wurtzite		
No. OPW's	r_m(3 Å)	r_m(5 Å)	r_m(7 Å)	No. OPW's	r_m(5 Å)	r_m(7 Å)
27	1.00	1.67	2.34	23	2.21	3.10
51	0.85	1.42	1.99	55	1.38	1.94
65	0.71	1.18	1.65	73	1.25	1.75
137	0.58	0.96	1.35	135	1.06	1.49
229	0.48	0.80	1.12	233	0.88	1.23
307	0.43	0.72	1.01	313	0.79	1.10
459	0.38	0.63	0.88	451	0.69	0.96
725	0.32	0.54	0.76	737	0.57	0.80
965	0.29	0.48	0.68	989	0.53	0.75

the bottom of the table by realizing that r_m is inversely proportional to the cube of the number of OPW's. This cubic dependence severely hampers OPW convergence.

The potential used by Herman and Skillman's OAP model is simply the superposition of the free-atom potentials of the atoms at their crystalline sites. Overlap is taken into account by means of the core shifts. In our SCOPW model, the OPW valence wave functions are used with the iterated-core wave functions to calculate the crystalline potential. In both cases, the Hartree-Fock exchange potential is approximated by either Slater's,[9] Kohn and Sham's,[10] or Liberman's[11] exchange approximation in which the exchange potential is taken to be proportional to the total electron density to the one-third power. In the SCOPW model, a fine crystalline mesh is used over which the total charge density is calculated. In Herman and Skillman's OAP model, the individual atomic charge densities are raised to the one-third power and then added. The Kohn-Sham exchange often gives slightly better band energies in Herman and Skillman's model, while Slater's exchange seems to give consistently good (i.e., agreeing with experiment) SCOPW energies without adjustments.[12] We expect the gross convergence properties examined in this paper to be insensitive to the exact form of exchange used. Slater's exchange is used throughout this paper.

Application of the variational principle to the bottom valence energy results in the matrix eigenvalue problem

$$H\psi = \lambda U\psi \ ,$$

where the positive definite Hermitian matrix U reflects the nonorthogonality of the OPW basis set. We solve this problem using a technique due to Shankland[6] which is especially useful for large matrices where diagonalization time is very important. One can easily decompose U into the product of a lower triangular matrix and its Hermitian adjoint

$$U = LL^{\dagger} \ ,$$

$$L_{ij} = 0, \text{ for } i < j \ .$$

The eigenvalue problem then reduces to

$$[L^{-1}HL^{-1\dagger}][L^{\dagger}\psi] = \lambda[L^{\dagger}\psi] \ ,$$

which requires only one diagonalization rather than two. The calculations of L and L^{-1} require only very short computer programs which are very fast. Because H and U are both Hermitian, they can be stored in the same matrix with only one additional array of diagonal elements being required.

III. CONVERGENCE

One's definition of convergence depends upon the accuracy with which one must know the band energies. In modern OPW calculations, this accuracy is about 0.02 eV. When we say that an energy is convergent, we mean that it is within 0.02 eV of the final flat value.

The Brillouin zone for the zinc-blende and diamond structure is shown in Fig. 2. Most of our interest is focused at the Γ, X, and L high-symmetry points. The variation of the SCOPW ZnS (Slater exchange, 229 OPW's) energy bands through the zone is shown in Fig. 3.

For this study, we will concentrate on the convergence of the Γ-point energies. Similar behavior is expected at the other zone points. Convergence studies of the X- and L-point energies of ZnO and BeTe will be presented to support this expectation. For convenience we will use the

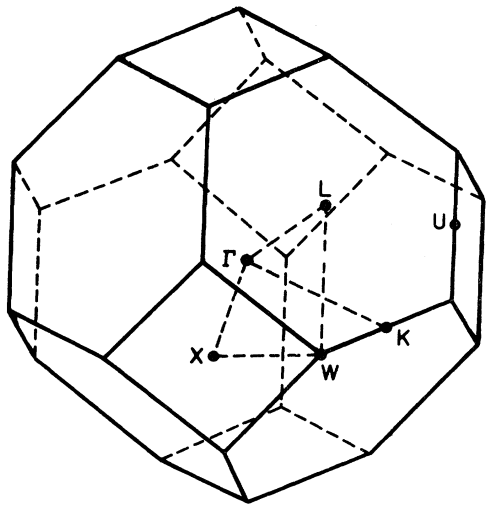

FIG. 2. Zinc-blende Brillouin zone. Important zone points for this paper are $\Gamma(0, 0, 0)$, $X(1, 0, 0)$, and $L(\frac{1}{2}, \frac{1}{2}, \frac{1}{2})$.

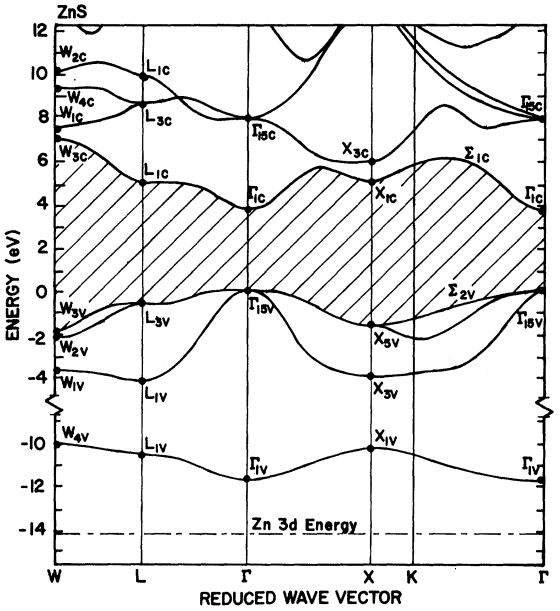

FIG. 3. ZnS SCOPW-229 OPW-Slater exchange bands are shown together with the position of the Zn 3*d* core energy. SCOPW high-symmetry point values are indicated by heavy dots. A pseudopotential interpolation scheme was used to generate the lines.

same notation for the Γ-point representations of the zinc-blende and diamond symmetries. The diamond and zinc-blende Γ_1 states are *s*-like in character and contain no core *p* states. In wurtzite symmetry, the Γ_1 splits into a Γ_1 and Γ_3. The diamond and zinc-blende Γ_{15} states are *p*-like and involve no core *s* states. In wurtzite structure, the Γ_{15} splits into a Γ_1, a Γ_3, a Γ_5, and a Γ_6.

Two primary factors are involved in OPW convergence. One is the well-known presence or absence of core wave functions of the particular band symmetry in the OPW's. For example, the first-row elements have no *p* states in their cores, and thus the Γ_{15} series is a pure plane-wave series rather than an OPW series. This factor has been discussed qualitatively by Callaway,[13] Heine,[14] and Herman.[15] We will present the results of several calculations which quantitatively show this effect. The other factor is the relative core size of anion and cation. For a given number of OPW's, r_m is proportional to the lattice constant, and consequently to the sum of the core radii. If one core radius is much smaller than the other, r_m will never get small enough to "feel out" the smaller core. By feel out, we mean adequately to represent the valence wave function in the core region.

Table II illustrates how we have tried to separate these two effects. The series C, Si, ZnSe, and CdTe shows the effect of no-core *p* states (one *s* state) through three-core *p* states (four-core *s* states) for equal-core sizes. The larger cation compounds and the larger anion compounds then show the effects of relative core size with and without core *p* states.

Figures 4 and 5 display the results of our convergence study. We have plotted in Fig. 4 the quantity

$$\sigma = 4\pi r^2 \rho$$

for the anion bottom valence free-atomic state on the same graph with the Γ_{1v} band energy, the *x* axis being *r* in one case and r_m in the other. The convergence behavior of the higher valence and conduction bands is shown in Fig. 5. Figure 5 also shows σ for the cation (heavy line) and the

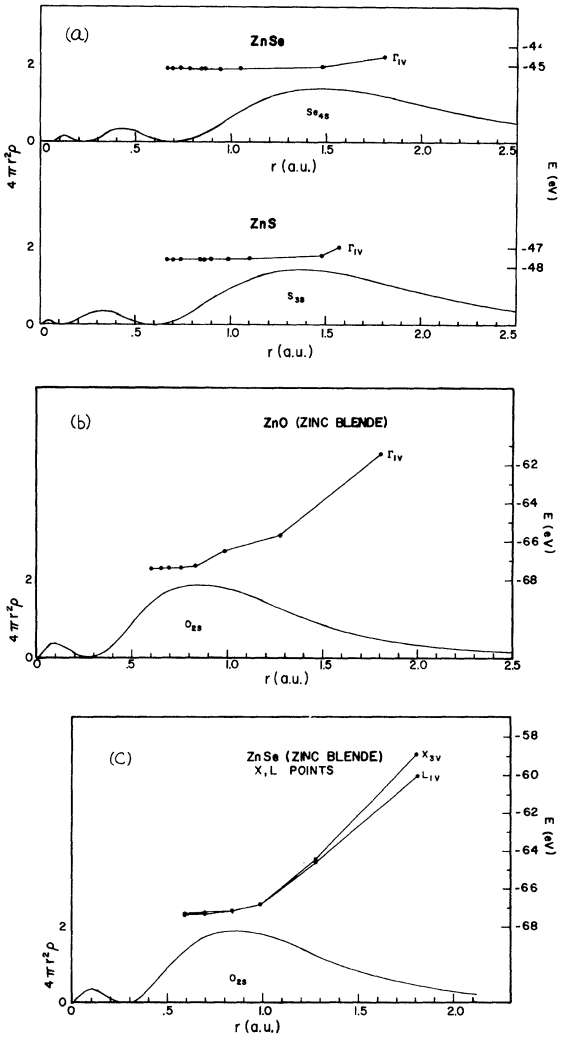

FIG. 4. Bottom valence-band energies are shown as a function of r_m. Charge density of the bottom valence-anion free-atom state is shown on the same plot.

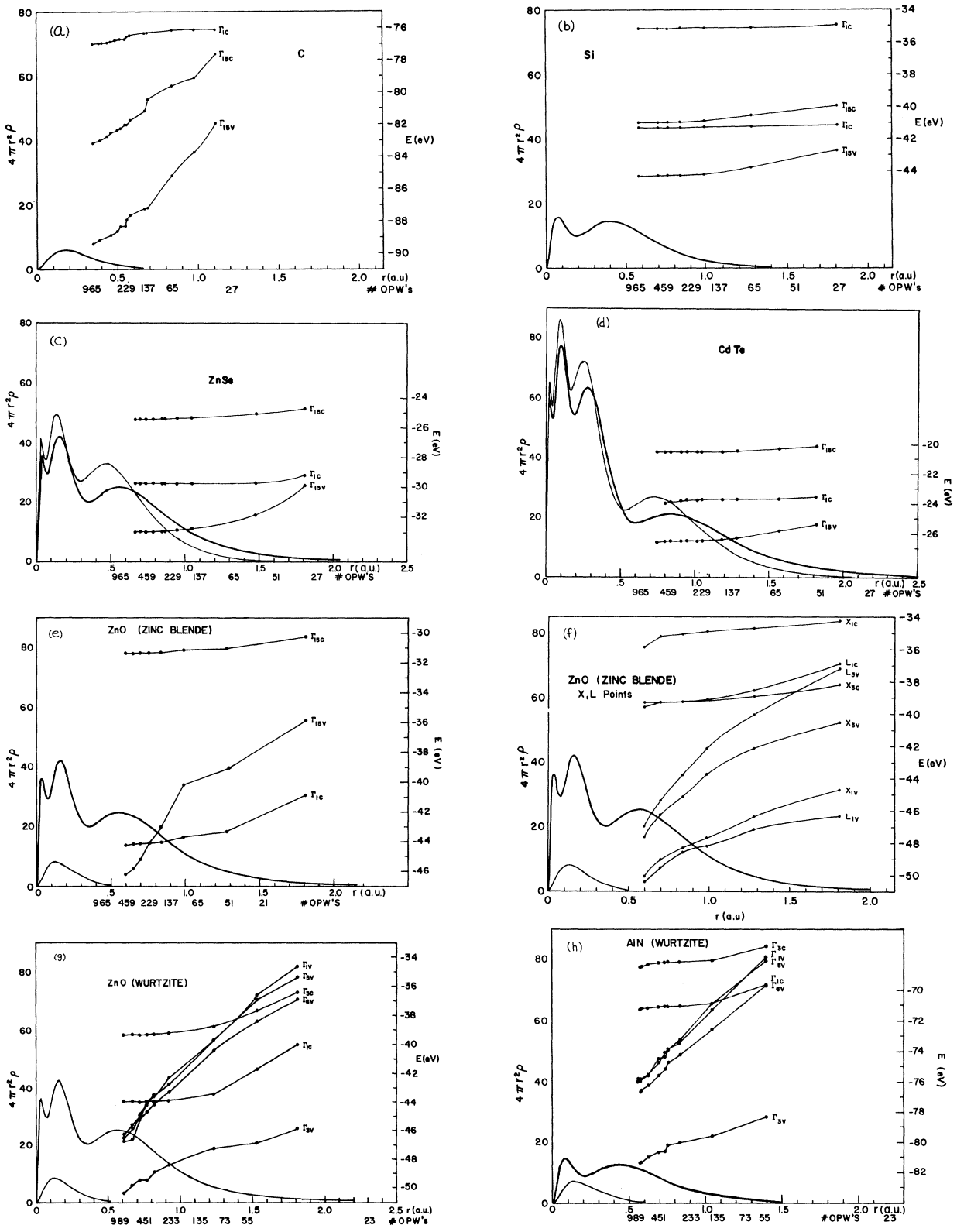

FIG. 5. Top valence bands and bottom conduction bands are plotted against r_m. Heavy dots show calculated values. On the same plot, anion and cation (heavier line) core charge densities are shown.

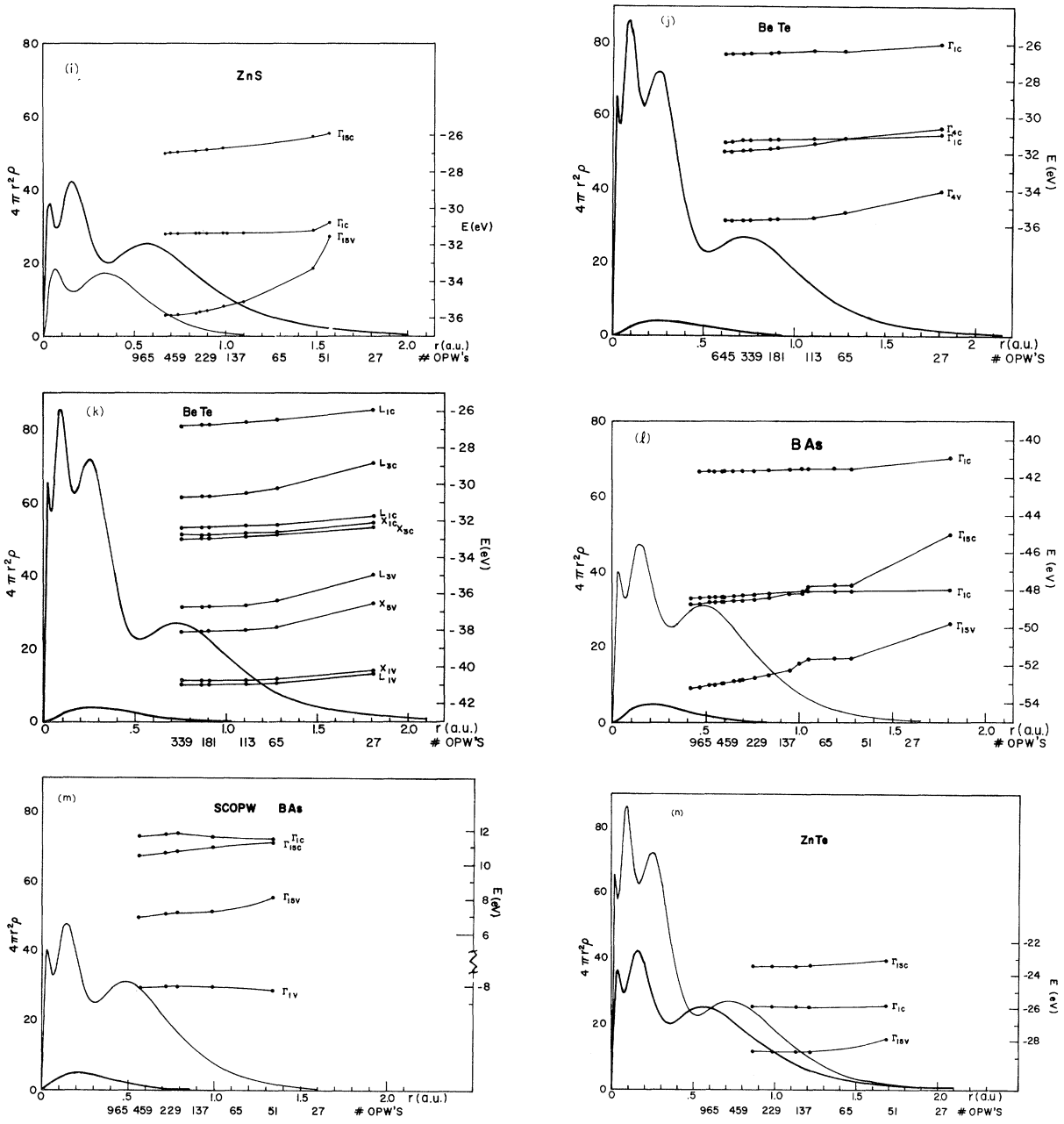

FIG. 5.(*Continued*).

anion cores. The X- and L-point behavior is shown for ZnO and BeTe. Self-consistent results are shown for BAs.

A. Convergence of Γ_{1v}

From the band diagram of Fig. 3, one sees that the bottom Γ_{1v} state varies relatively little throughout the Brillouin zone. Hence this band resembles a core state, which is assumed to be perfectly flat throughout the zone. In fact, from a comparison of free-atom (plus core-shift) energies with the band energy, it can be seen that this bottom Γ_1 is very similar to the bottom anion valence s state. For example, in sulfides it corresponds closely to the S $3s$ state.

The most dramatic convergence effects are seen for ZnO where the anion is small, and consequently the bottom valence s state for a free atom is also relatively small. But the effect is also clearly visible in ZnS and ZnSe. Over-all convergence is

obtained when r_m is equal to the radius at which σ is a maximum, although there is occasionally some slight falloff beyond this point. The X- and L-point convergence is slightly slower, but substantially the same. This convergence behavior supports our choice of r_m as a proper distance measure for our further considerations.

B. Dependence on Number of Core-State Functions in OPW's

First we consider the equal-core compounds. The C core consists of a single s state. The Γ_{1v} (which involves this $1s$ state) has relatively good convergence. Where r_m equals the radius at which σ equals $\frac{1}{3}$ of its maximum, convergence is complete. This is at around 700 OPW's. The C Γ_{15} have no core states to aid convergence. The OPW series becomes a plane-wave series – a straight Fourier series. Convergence is very slow. We suspect that relatively complete Γ_{15} convergence for C would require an r_m of about 5000 plane waves. The contrast between the C and Si convergence is dramatic. Si has both $1s$ core states to aid the Γ_1 convergence, and it has a $2p$ core state to aid the Γ_{15} convergence. The Γ_{1c} state has obtained complete convergence at about $\frac{1}{5}\sigma_{\max}$.

The Si Γ_{15} convergence is comparable to the C Γ_{1c} convergence which is significant since they both have one core state. As in the case of the C Γ_{1c} state, convergence of the Si Γ_{15} is obtained at about $\frac{1}{3}\sigma_{\max}$. ZnSe and CdTe convergence is very good. In each case, convergence is about complete by $\frac{1}{5}\sigma_{\max}$.

Looking at the Zn sequence from ZnO through ZnTe, we note progressively better convergence as the anion core becomes richer in orthogonalization states. This qualitative behavior was, of course, pointed out long ago by previous workers.

C. Dependence of Γ_{15v} on Anion Core Size

Γ_{15} convergence is worst for the large-cation–small-anion compounds. In both ZnO and AlN, the Γ_{15v} valence state is above the Γ_{1c} conduction state at large r_m. The Γ_{15v} convergence clearly depends critically upon the anion core size. In ZnS, Γ_{15v} convergence will be complete at around $\frac{1}{3}\sigma_{\max}$ for the anion core. Note that S has a single-core p state to aid convergence. The Γ_{15v} convergence is much better for the large-anion–small-cation compounds, substantiating the strong dependence upon anion size. For example, in BAs and BeTe, the Γ_{15} curves are flatter than for ZnO and AlN. There is a leveling off as the anion core is penetrated, but a significant further lowering as the cation core (containing no p state) is penetrated. In ZnTe, the Γ_{15v} and Γ_{15c} both level off at about $\frac{1}{7}\sigma_{\max}$. This occurs at roughly the same point for both anion and cation for ZnTe.

The behavior of the X- and L-point top valence bands is shown for cubic ZnO and BeTe. Again, the ZnO valence bands go down much more steeply than the BeTe bands, showing the critical dependence of the p-like valence bands upon the anion size.

We can see from these figures that the convergence of the top valence band depends critically upon the anion core size, with a weaker dependence upon the cation core size. Convergence seems to be complete when the smaller core is penetrated to $\frac{1}{3}\sigma_{\max}$ if the core contains one p state and by $\frac{1}{5}\sigma_{\max}$ if the core contains more than one p state. If either core contains no p states, convergence is very poor.

D. Dependence of Γ_{1c} on Cation Core Size

In the large-cation–small-anion compounds, ZnO, AlN, and ZnS, the Γ_{1c} band can be seen to level off almost completely when the cation core is penetrated to $\frac{1}{3}\sigma_{\max}$ for ZnO and AlN and $\frac{1}{8}\sigma_{\max}$ for ZnS. This is in contrast to the large-anion–small-cation compounds BAs and BeTe where there is a significant falloff of the Γ_{1c} even when the large-anion core is well penetrated. Clearly, the Γ_{1c} convergence depends almost completely upon the cation core size. Any dependence upon the anion size is less obvious than the Γ_{15v} dependence upon cation size because all cores contain at least one s state to aid the convergence.

E. SCOPW Convergence

In our experience, SCOPW convergence seems to be just slightly better than OAP convergence. But the over-all features are the same. One cannot count on self-consistency significantly to improve poor convergence. (We tried this on ZnO.) As an example of SCOPW convergence, we show results for BAs in Fig. 5. It will be noted that the addition of more OPW's does not always lower the self-consistent bands as it does the OAP bands. This is because the SCOPW potential changes with r_m. The familiar variational behavior is thus seen only for the OAP results.

IV. CONCLUSIONS

Two factors are relevant for OPW convergence. One is the number of core-state functions contained in the OPW's. The presence of even one core-state function helps dramatically as was seen for Si compared with C. The other factor is the relative core sizes of anion and cation. For a given number of OPW's, r_m is proportional to the sum of the core radii, while convergence depends upon the penetration into the smaller core. As a rough

rule of thumb, with one core function in an OPW, one must penetrate to about $\frac{1}{3}\sigma_{max}$. With more than one core function in an OPW, one must penetrate to about $\frac{1}{5}\sigma_{max}$. The Γ_{1v} convergence can be judged from the free-atom anion bottom valence state maximum in σ. The Γ_{15v} convergence depends more strongly on the anion core size, with some dependence on the cation size. The Γ_{1c} convergence depends very strongly on the cation size. Convergence is similar throughout the zone. The fact that the OPW's must penetrate the smaller core is a major weakness in the OPW formalism. However, beyond the first row of the Periodic Table, the OPW formalism seems adequate to handle any compound if pseudocore states are introduced to handle such things as high-lying d states.[3,13,16,17]

ACKNOWLEDGMENTS

We would like to thank R. Schultz who programmed a large diagonalization procedure for us. We are also grateful to G. Johnson and G. Schantz for their expert drafting of the many figures.

[1]J. C. Slater, Phys. Rev. 51, 846 (1937).
[2]W. Kohn and W. Rostoker, Phys. Rev. 94, 1111 (1954).
[3]C. Herring, Phys. Rev. 57, 1169 (1940).
[4]T. O. Woodruff, in *Solid State Physics*, edited by F. Seitz and D. Turnbull (Academic, New York, 1957), Vol. V, p. 367.
[5]F. Herman and S. Skillman, in *Proceedings of the International Conference on Semiconductors Physics, Prague*, 1960 (Publishing House of Czechoslovak Academy of Science, Prague, 1961), p. 20.
[6]R. N. Euwema, T. C. Collins, D. G. Shankland, and J. S. DeWitt, Phys. Rev. 162, 710 (1967).
[7]D. J. Stukel, R. N. Euwema, T. C. Collins, F. Herman, and R. K. Kortum, Phys. Rev. 179, 740 (1969).
[8]F. Herman and S. Skillman, *Atomic Structure Calculations* (Prentice-Hall, Englewood Cliffs, N. J., 1963).
[9]J. C. Slater, Phys. Rev. 81, 385 (1951).
[10]W. Kohn and L. J. Sham, Phys. Rev. 140, A1133 (1965).
[11]D. A. Liberman, Phys. Rev. 171, 1 (1968).
[12]D. J. Stukel, R. N. Euwema, T. C. Collins, and V. Smith, Phys. Rev. B1, 779 (1970).
[13]J. Callaway, Phys. Rev. 97, 933 (1955).
[14]V. Heine, Proc. Roy. Soc. (London) A240, 340 (1957); A240, 354 (1957); A240, 361 (1957).
[15]F. Herman, Phys. Rev. 93, 1214 (1954).
[16]R. A. Deegan and W. D. Twose, Phys. Rev. 164, 993 (1967).
[17]F. A. Butler, F. K. Bloom, and E. Brown, Phys. Rev. 180, 744 (1969).

PHYSICAL REVIEW B VOLUME 1, NUMBER 12 15 JUNE 1970

New Ordered Phases of Slightly Reduced Rutile and Their Sharp Dielectric Absorptions at Low Temperature

C. W. Chu
Bell Telephone Laboratories, Murray Hill, New Jersey 07974
(Received 2 December 1969)

The temperature dependence of the complex dielectric constant of single-crystal rutile has been studied at different frequencies and as a function of reduction. The results suggest the existence of two new ordered phases in slightly reduced rutile. Sharp dielectric absorptions have been observed in these phases. This is attributed to the hopping of low-mobility charge carriers between two ion sites. The nature of the charge carriers introduced by reduction is discussed. It is proposed that the room-temperature conductivity alone may not characterize the state of a slightly reduced rutile sample.

INTRODUCTION

Metal-nonmetal transitions in transition-metal[1] oxides have long received intense interest. The recent identification[2] of a Mott transition in Cr-doped V_2O_3 is one of its highlights. With this point in view as well and considering the anomalously high dielectric constant ($\epsilon = 173$)[3] of rutile (TiO_2), the study of stoichiometric and reduced rutile is instructive in the understanding of the electrical-transport mechanism in rutile.

Stoichiometric rutile is a highly polar insulating crystal with an intrinsic energy gap[4] ~3 eV between the filled $2p$ band of O^{-2} and the empty $3d$ band of Ti^{+4}. Slight reduction of rutile by heating in vacuum